

Wind-Powered Centrifugal Pump System: Investigating the Potential for Removing the Interfacing Converter Stabilizer

Saci Taraft^{1*}✉, Djamal Aouzellag¹ and Farid Hamoudi¹

¹Laboratory of Renewable Energy Mastery, University of Bejaia, 06000, Algeria

✉ taraft1@hotmail.com

Abstract

Population growth has led to a significant increase in demand for water resources. The scarcity of surface water has made tapping into available groundwater resources essential. This article presents a study focusing on water pumping using a less cumbersome wind system with improved efficiency. This is achieved by eliminating the power electronics interface and its control, which in turn removes harmonics generated by the static converter and requires less maintenance. The simulation results are compared with those from similar systems that include the power electronics bay.

Keywords: Wind-turbine, Static converters, PMSG-IM, Centrifugal-Pump, Passive Stall.

Nomenclature:

S_i - rectifier and inverter switch,
PMSG - Permanent Magnet Synchronous Generator,
IM - Induction machine,
DC AC - Direct and alternative current,
SC - Static Converter
PWM - Pulse Wide Modulation,
MPPT - Maximum Power Point Tracking,
 V_{wind} - wind speed, $m.s^{-1}$,
 T_t - turbine torque, N.m,
 P_{wind} - wind power, W,
 S - area, m^2 ,
 P_t - turbine power, W,
 R - blade radius, m,
 $V_d V_q$ - PMSG, direct and quadratic voltage, V,

$i_d i_q$ - PMSG, direct and quadratic current, A,
 r - PMSG, stator resistance, ohm,
 $L_d L_q$ - PMSG, stator direct and quadratic inductance, H,
 $T_{em} T_{em_IM}$ - PMSG and IM electromagnetic torque, N.m,
 $P_1 P_2$ - PMSG and IM peer poles respectively,
 f - viscous friction coefficient,
 $V_{sd} V_{sq}$ - IM, direct and quadratic voltage, V,
 $r_s r_r$ - IM, stator and rotor resistance, ohm,
 w - IM, electrical speed, rad/s,
 $L_s L_r$ - IM, stator and rotor inductance, H,
 M - IM mutual, H,
 $i_{sd} i_{sq}$ - IM, stator direct and quadratic current, A,
 $i_{rd} i_{rq}$ - IM, rotor direct and quadratic current, A,
 T_r - pump resistant torque, N.m,
 K_r - pump torque coefficient, $N.m.s^2.rad^{-2}$,
 P_m - pump mechanical power, W,
 P_h - hydro power, W,
 g - gravitational acceleration, $m.s^{-2}$,
 P_{IM} - IM active power, W,
 V_{dc} - DC voltage,
 C - capacitor, F,
 $i_{rec} i_{inv}$ - rectifier and inverter current, A,
 i_c - capacitor current, A,
 $J_t J_p$ - inertia of the turbine and the pump respectively, $Kg.m^2$,
 P_{pump} - Pump active power, W,



$P_{sg}P_{sg_ref}$ - PMSG electrical active power and it's reference, W,

T_{r_IM} - IM resistant torque, N.m.

1. Introduction

Demographic growth and agropastoral development are continuously increasing, with a significant impact on the demand for water. Consequently, the scarcity of surface water has led researchers to design systems for extracting available underground water. In order to contribute to the purification of the atmosphere, it is essential to use energy from renewable sources. These sources are exploited in several applications, such as powering remote locations, pumping, and more. Numerous works have been developed on techniques and strategies for producing electrical energy from wind power, which is applied to supply both autonomous loads and loads connected to the electrical grid. Wind pumping is now becoming more attractive than traditional mechanical pumping [1] due to several advantages it offers over mechanical pumping [2]. A non-linear control is applied in [3] to optimize wind power production. In [4], an optimization algorithm is used in a wind energy system for reactive power management at the input and output of the converter. In [5], a new technique is presented for setting the active power injected into the electrical grid and correcting the power factor using reactive power produced by the generator. The control of wind power generation to adapt it to the requirements of an autonomous system is presented in [6]. In reference [7], energy production regulation is ensured using the active stall technique by actuating half of the blade; however, this technique requires integrating actuators, making control more complex. Another interesting wind pumping proposal in [8] involves eliminating static converters; on the other hand, the drawn water is used only for producing electrical power. In these works, it is observed that the power flow from the wind source to the load passes through a power electronics interface. However, this

solution is expensive and typically requires proper control. Furthermore, this converter is often the source of harmonics that impair the proper functioning of the system and necessitate well-adapted filters. This article presents a model of wind pumping operating in two zones:

- Zone where the maximum power extraction algorithm is applied (MPPT).
- Zone where power limitation is achieved through passive release of the blades (Stall-control).

On one hand, the study is conducted with the use of a power electronics interface; on the other hand, it explores the possibility of eliminating the power electronics interface by leveraging the characteristics and appropriate selection of the centrifugal pump. This paper is primarily divided into two parts: The first part is devoted to describing the studied system, the mathematical models governing the operation of the pumping system and presenting the flux-oriented control. Meanwhile, the second part presents the model and investigates the possibility of eliminating the power electronics bay in a wind pumping system by exploiting the torque-speed characteristic of the centrifugal-type pump.

Table 1: Basic parameters of PMSG

Designation	Value
Stator winding resistance	4.90 Ω
Direct cyclic inductance	25 mH
Quadratic cyclic inductance	25 mH
Excitation Flux	0.7Wb

Simulation results with and without the power electronics bay are ultimately presented and discussed.

1.1. Description of the studied system

The system under study consists of a passive stall wind turbine that rotationally drives a permanent magnet synchronous generator. This



generator powers an induction motor, which in turn drives a centrifugal pump. The motor pump is supplied in two different ways: first, through a power electronics bay; and second, directly from the synchronous generator without a power converter. The machines operate in a master-slave configuration. The overall schematic of the studied model is depicted in Figure 1.

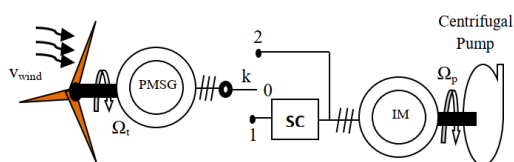


Figure 1: Global synoptic diagram of the studied system

1.2. Different parts modeling of the pumping system

1.2.1. Turbine modeling

The turbine in question is of the three-bladed type, driven by the force of the wind, as illustrated in Figure Figure 2.

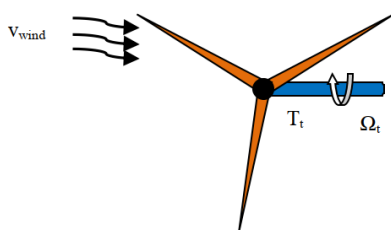


Figure 2: Wind turbine

The wind power available in a cylinder of section S is given by [13]:

$$P_{wind} = \frac{1}{2} \rho S v_{wind}^3 \quad (1)$$

Where ρ is the air density (dry atmospheric air, approximately 1.225 kg/m^3 at 15°C and 1.0132 bar atmospheric pressure); S is the wind sensor surface. In the case of a propeller of length R , the available wind power is proportional to the square of the length of the blade and to the cube

of the wind speed. The power captured by the wind turbine is given by [10]:

$$P_t = \frac{1}{2} \rho S C_p(\lambda, \beta) \cdot v_{wind}^3 \quad (2)$$

Where C_p is a coefficient characterizing the aerodynamic efficiency of the turbine that depends on the dimensions of the blade, the specific speed λ and the pitch angle β . In this article, the blade is a passive stall type. Therefore, the turbine is independent of the pitch angle β . Evolution of the (optimal) mechanical power recovered as a function of the wind speed is shown in Figure Figure 3.

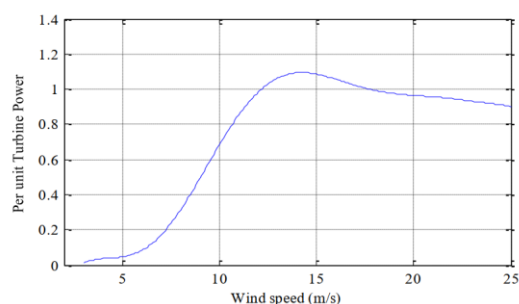


Figure 3: Aerodynamic Turbine Power versus Wind Speed

The specific speed λ is defined as the ratio between the linear speed at the tips of the blades and the wind speed. Its expression is defined by the following relation:

$$\lambda = \frac{R\Omega_t}{v_{wind}} \quad (3)$$

The mechanical torque developed by the wind turbine is defined as the ratio between the power captured and the rotation speed of the wind turbine; the relation between these physical graders is given by [14]:

$$T_t = \frac{P_t}{\Omega_t} \quad (4)$$

1.2.2 Permanent magnet generator modeling

The synchronous machine is chosen according to its advantages, namely: absence of brushes and



reduced losses compared to another asynchronous and wound rotor synchronous machine. In addition to its high specific torque and easy control (non-estimated flux). The representation of the permanent magnet machine in the virtual coordinate system (d, q) is illustrated in Figure 4.

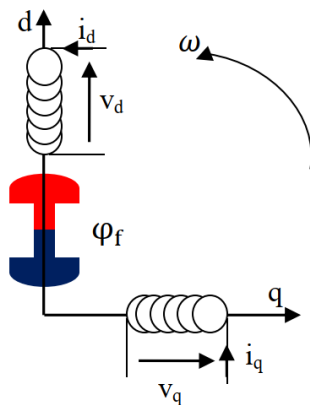


Figure 4: Representation of PMSM in the landmarks (d, q)

1.2.3 Electrical equations

The voltage equations of the PMSG in the Park coordinate system linked to the rotor are:

$$\begin{cases} V_d = r i_d + \frac{d\varphi_d}{dt} - p_1 \Omega_t \varphi_q \\ V_q = r i_q + \frac{d\varphi_q}{dt} + p_1 \Omega_t \varphi_d \end{cases} \quad (5)$$

1.2.4 Magnetic equations

The flux on the direct and quadratic axis φ_d and φ_q respectively are given by the following system of equations [11]

$$\begin{cases} \varphi_d = L_d i_d + \varphi_f \\ \varphi_q = L_q i_q \end{cases} \quad (6)$$

With: φ_f is a constant flux created by the rotor magnets.

1.2.5 Electromagnetic torque

The electromagnetic torque T_{em} is produced by the interaction between the magnetic poles of the rotor and the poles generated by the

magneto motive forces (fmm) in the air gap resulting from the stator currents. This torque is expressed as:

$$T_{em} = p_1 [(L_d - L_q) i_d i_q + i_q \varphi_f] \quad (7)$$

1.2.6 Mechanical equation

The mechanical equation is expressed as follows:

$$J \frac{d\Omega_t}{dt} + f \Omega_t = T_t - T_{em} \quad (8)$$

1.3. Asynchronous motor modeling

1.3.1 Electrical equations

The expressions of the electric voltages in Park's fictitious reference frames (d, q) are given by the systems of equations (9) and (10)

$$\begin{cases} V_{sd} = r_s i_{sd} + \frac{d\varphi_{sd}}{dt} - \omega \varphi_{sq} \\ V_{sq} = r_s i_{sq} + \frac{d\varphi_{sq}}{dt} + \omega \varphi_{sd} \end{cases} \quad (9)$$

$$\begin{cases} V_{rd} = 0 = r_r i_{rd} + \frac{d\varphi_{rd}}{dt} - (\omega - \omega_r) \varphi_{rq} \\ V_{rq} = 0 = r_r i_{rq} + \frac{d\varphi_{rq}}{dt} + (\omega - \omega_r) \varphi_{rd} \end{cases} \quad (10)$$

1.3.2 Magnetic equations

The stator and rotor fluxes in the Park coordinate system are expressed by the following matrix relation:

$$\begin{bmatrix} j_{sd} \\ j_{sq} \\ j_{rd} \\ j_{rq} \end{bmatrix} = \begin{bmatrix} L_s & 0 & M & 0 \\ 0 & L_s & 0 & M \\ M & 0 & L_r & 0 \\ 0 & M & 0 & L_r \end{bmatrix} \begin{bmatrix} i_{sd} \\ i_{sq} \\ i_{rd} \\ i_{rq} \end{bmatrix} \quad (11)$$

The expression of the electromagnetic torque as a function of the rotor flux and stator currents is as follows:

$$T_{em_IM} = \frac{P_2 M}{L_r} = (j_{rd} i_{sq} - j_{rq} i_{sd}) \quad (12)$$



1.4. Centrifugal pump modeling

The resistant torque and the mechanical power on the shaft of the centrifugal pump are given by the following system of equations:

$$\begin{cases} T_r = K_r W_p^2 \\ P_m = K_r W_p^3 \end{cases} \quad (13)$$

The flow of water drawn at a manometric head H_m is expressed by [9] [12]:

$$Q = \frac{P_h}{P_w g H_m} \quad (14)$$

$$P_h = h_p P_m \quad (15)$$

Where: h_p is the pump efficiency, P_m is the mechanical power and g is the gravitational acceleration, $m.s^{-2}$

The torque characteristic as a function of the rotation speed of the studied pump is illustrated in Figure Figure 5.

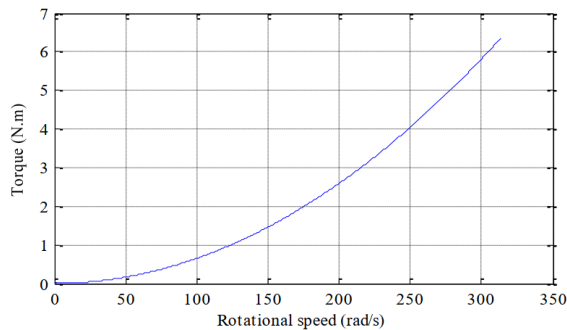


Figure 5: Pump torque versus rotational Speed

1.5. Power electronic bay modeling

The power electronics bay used is a cascaded PWM inverter-filter rectifier. The assembly is shown in Fig.Figure 6.

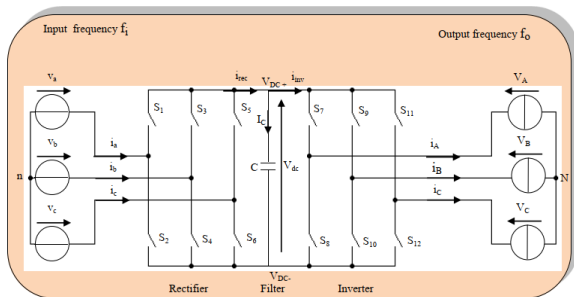


Figure 6: Back-to-Back Converter

1.5.1. PWM rectifier modeling

Using the connection functions S_i , $i = 1$ to 6, for each rectifier switch, the transfer matrix from AC to DC is defined as follows [15]:

$$\begin{bmatrix} V_{DC+} \\ V_{DC-} \end{bmatrix} = \begin{bmatrix} S_1 & S_3 & S_5 \\ S_2 & S_4 & S_6 \end{bmatrix} \begin{bmatrix} V_a \\ V_b \\ V_c \end{bmatrix} \quad (16)$$

and

$$V_{dc} = V_{DC+} - V_{DC-} \quad (17)$$

The rectified current according to the input currents is given by the expression (18):

$$i_{rec} = [s_1 s_3 s_5] \begin{bmatrix} i_a \\ i_b \\ i_c \end{bmatrix} \quad (18)$$

1.5.2. Filter modeling

The filter used in this article is a low-pass type shown in Figure Figure 7.

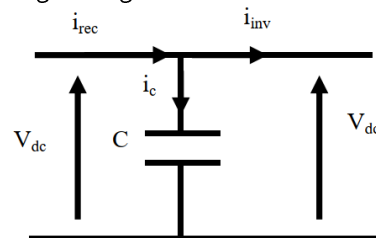


Figure 7: Representation of a low-pass filter

The filter model is defined by the following system of equations:

$$\begin{cases} i_{rec} - i_{inv} = C \frac{dv_{dc}}{dt} \\ v_{dc}(t) = v_{dc}(0) + \frac{1}{C} \int_{t-1}^{t_2} (i_{rec} - i_{inv}) dt \end{cases} \quad (19)$$

The role of capacitor C is to ensure a voltage source character at the inverter input.



1.5.3. Inverter modeling

The voltage inverter provides the power conversion from DC form to AC form. The output voltages are governed by expression (20).

$$\begin{bmatrix} V_a \\ V_b \\ V_c \end{bmatrix} = \frac{V_{dc}}{3} \begin{bmatrix} 2 & -1 & -1 \\ -1 & 2 & -1 \\ -1 & -1 & 2 \end{bmatrix} \begin{bmatrix} S_7 \\ S_9 \\ S_{11} \end{bmatrix} \quad (20)$$

With S_i , $i = 7$ to 12 , is connection function associated to each switch in the inverter. For the two converters, the PWM control technique is applied.

2. Vector control of the two machines

The vector control of the AC machine consists of bringing its behavior to that of separately excited DC machine.

2.1. Permanent magnet generator control

To achieve a control similar to that of separately excited DC machine, it is necessary to keep the current i_d to zero, and to regulate the speed by current i_q through voltage v_q .

The system of equations (5) becomes:

$$\begin{cases} v_d = -p_1 W_t L_q i_q \\ v_q = (r + sL_q) i_q + p_1 W_t j_f \end{cases} \quad (21)$$

2.2. Induction machine control

The rotor flux orientation leads to control independently the current and flux to impose the torque.

$$\begin{cases} j_{rd} = j_r \\ j_{rq} = 0 \end{cases} \quad (22)$$

From these considerations, the expression of the electromagnetic torque (12) becomes:

$$T_{em_IM} = \frac{P_2 M}{L_r} = (j_{rd} i_{sq}) \quad (23)$$

The expressions of rotor voltages (10) become:

$$\begin{cases} 0 = r_r i_{rd} + \frac{dj_r}{dt} \\ 0 = r_r i_{rq} + (w + w_r) j_r \end{cases} \quad (24)$$

From the matrix form (11) and the system of equations (24), the rotor flux is obtained in Laplace plane as given in (25):

$$w_r = \frac{M}{[1 + stt_r]} i_{sd} \quad (25)$$

With: t_r is the rotor time constant given as $t_r = \frac{L_r}{R_r}$.

The rotor flux is almost equal to the stator flux

$$j_r \gg j_s \quad (26)$$

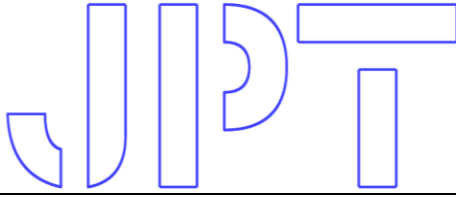
3. Study of the elimination possibility of the static converter

By substituting the system of equations (6) in (5) and the system of equations (11) in (9) and (10), the systems of equations (27) and (28) are deduced:

$$\text{PMSG:} \begin{cases} V_d = r i_d + L_d \frac{di_d}{dt} - p_1 W_t L_q i_q \\ v_q = r i_q + L_d \frac{di_q}{dt} + L_d i_d p_1 W_t + p_1 W_t j_f \end{cases} \quad (27)$$

$$\text{IM:} \begin{cases} V_{sd} = r_s i_{sd} + L_s \frac{di_{sd}}{dt} + M \frac{di_{rd}}{dt} - w(L_s i_{sq} + M i_{rq}); \\ V_{sq} = r_s i_{sq} + L_s \frac{di_{sq}}{dt} + M \frac{di_{rq}}{dt} - w(L_s i_{sd} + M i_{rd}); \\ 0 = r_r i_{rd} + M \frac{di_{sd}}{dt} + L_r \frac{di_{rd}}{dt} - (w - w_r)(M i_{sq} + L_r i_{rq}); \\ 0 = r_r i_{rq} + M \frac{di_{sq}}{dt} + L_r \frac{di_{rq}}{dt} - (w - w_r)(M i_{sd} + L_r i_{rd}). \end{cases} \quad (28)$$

With $w = p_1 W_t$ is the speed of rotating reference frames linked to the PMSG rotor; $w_r = p_2 W_p$ is the IM electric rotor speed; p_1 and p_2 are number of pair of poles of PMSG and IM



$$\left\{ \begin{array}{l} V_d = r i_d + L_d \frac{di_d}{dt} - p_1 W_t L_q i_q; \\ V_q = r i_q + L_q \frac{d}{dt} i_q + p_1 W_t (L_d i_d + j_f); \\ V_d = -r_s i_d - L_s \frac{di_d}{dt} + M \frac{di_{rd}}{dt} \\ \quad w(-L_s i_q + M i_{rq}); \\ V_{dq} = -r_s i_{dq} - L_s \frac{di_q}{dt} + M \frac{di_{rq}}{dt} \\ \quad w(-L_s i_d + M i_{rd}); \\ 0 = r_r i_{rd} - M \frac{di_d}{dt} + L_r \frac{di_{rd}}{dt} + \\ \quad (w - w_r)(-M i_q + L_r i_{rq}); \\ 0 = r_r i_{rq} - M \frac{di_q}{dt} + L_r \frac{di_{rq}}{dt} + \\ \quad (w - w_r)(-M i_d + L_r i_{rd}). \end{array} \right. \quad (30)$$

respectively; finally, t and p indices represent the turbine and pump, respectively.

In order to eliminate the static converter and make an electrical coupling between the synchronous and asynchronous machines, proceed as follows:

$$\left\{ \begin{array}{l} V_{ds} = V_d \\ V_{qs} = V_q \\ i_{sd} = -i_d \\ i_{sq} = -i_q \end{array} \right. \quad (29)$$

By substituting the currents expressed in the system of equations (29) in the systems of equations (27) and (28), the system of equations (30) is obtained

Table 2: Basic parameters of IM

Designation		Value
Stator winding resistance		4.80 Ω
Rotor winding resistance		3.71 Ω
Stator cyclic inductance		0.280 H

Rotor cyclic inductance		0.280 H
Mutual inductance		0.260 H
Inertia		0.031 kg.m3
Friction coefficient		0.00114 N.m.s.rad-1

After some simplifications and inserting the two mechanical equations of the turbine and the pump, the model of the system without power electronic converter is written as follows. Where:

$T_{em} = p_1 [(L_d - L_q) i_d i_q + i_q j_f]$ represents PMSG the electromagnetic torque,

$T_{em_IM} = p_2 M (i_{sq} i_{rd} - i_{sd} i_{rq}) = p_2 M (i_d i_{rq} - i_q i_{rd})$ the electromagnetic torque.

$$\left\{ \begin{array}{l} 0 = (r + r_s) i_d + (L_d + L_s) \frac{di_d}{dt} - p_1 W_t \\ \quad [(L_q + L_s) i_q - M i_{rq}] - M \frac{di_{rd}}{dt}; \\ 0 = (r + r_s) i_q + (L_q + L_s) \frac{di_q}{dt} - p_1 W_t \\ \quad [(L_{qd} + L_s) i_d - M i_{rd} + j_f] - M \frac{di_{rq}}{dt}; \\ 0 = r_r i_{rd} - M \frac{di_d}{dt} + L_r \frac{di_{rd}}{dt} - \\ \quad (p_1 W_t - p_2 W_t)(-M i_q + L_r i_{rq}); \\ 0 = r_r i_{rq} - M \frac{di_q}{dt} + L_r \frac{di_{rq}}{dt} - \\ \quad (p_1 W_t - p_2 W_t)(-M i_d + L_r i_{rd}); \\ J_t \frac{dW_t}{dt} + f_t W_t = T_t - T_{em}; \\ J_p \frac{dW_p}{dt} = T_{em_IM} - T_{r_IM} - f_p W_p \end{array} \right. \quad (31)$$

4. Simulation results

Simulation results were obtained with a permanent magnet machine of 2.3 kW rated power. The latter is driven by a passive stall wind turbine. The centrifugal pump is driven by



a 2kW rated power induction machine. This one is supplied as follows:

- 1 - By the synchronous generator through the power electronics bay,
- 2 - By the same generator, with eliminating of the power electronics bay.

The simulation results of the dynamic behavior of the studied system, with and without the static converter are shown in figures ranging from 8 to 27.

In figure 8 the wind profile used in both wind pumping models is shown, namely with and without the presence of the power electronics bay.

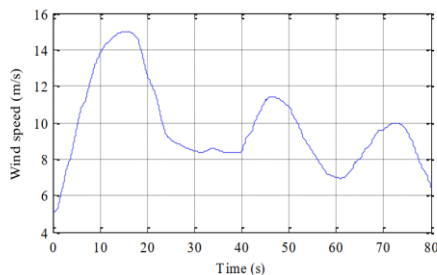


Figure 8: Profile of the Wind speed

4.1. With power electronics bay

In this section, simulation results of wind pumping model with the presence of the static converter are shown in figures from 9 to 19. Turbine rotational speed and its reference are shown in Figure Figure 9.

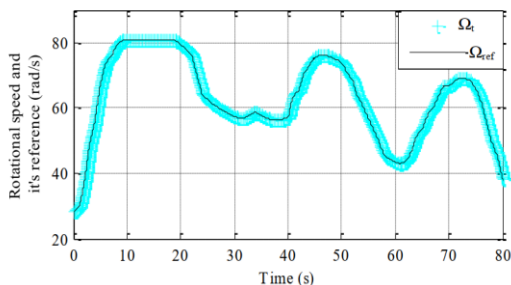


Figure 9: Rotational speed of the PMSG

The mechanical power developed by the turbine is shown in Figure Figure 10; this power is limited to an allowable value (passive stall) as shown in the interval from 8 to 22 seconds.

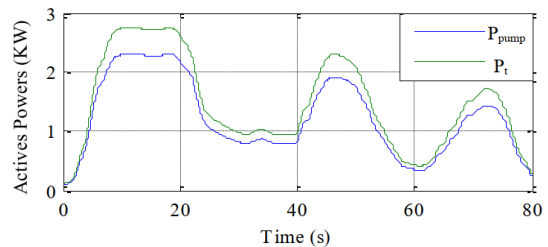


Figure 10: Active Power of the Centrifugal Pump and wind Turbine

The electric power generated by the PMSG illustrated in Figure Figure 11, follows its reference which is evaluated by $P_{s_ref} = -h_G P_t$. This also applies to the direct currents forced to zero by the control, while the in quadratic current follows its reference, which given from the speed regulator as illustrates Figure Figure 12. This can justify the reliability of the control.

The electromagnetic torque developed by the PMSG is shown in Figure Figure 13; this torque is the image of the quadratic current i_q .

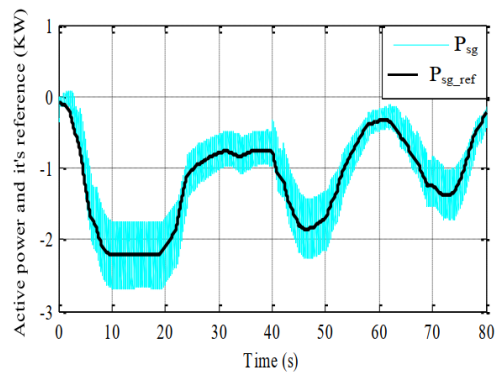


Figure 11: Active power and its reference of PMSG

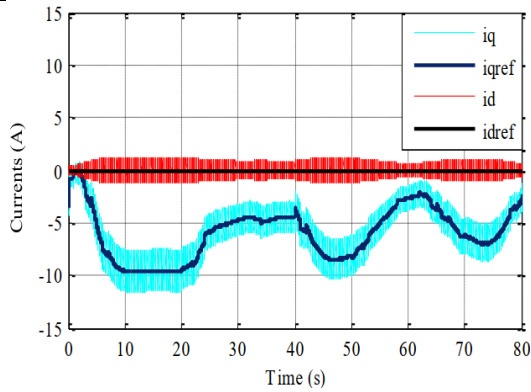


Figure 12: Direct, quadratic currents and its reference of PMSG

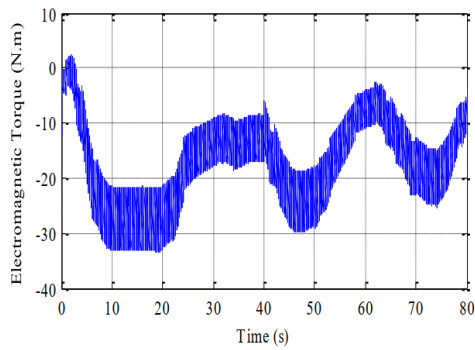


Figure 13: Electromagnetic Torque

The voltage and current of the same phase are shown in Figure Figure 14, zooming over a period clearly shows the generator mode operation of the PMSG.

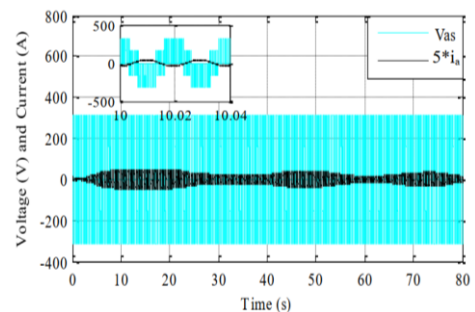


Figure 14: Voltage and Current of the PMSG

In Figure Figure 15, the IM rotation speed faithfully follows its reference, which justifies the reliability of the control. The

electromagnetic and resistive torques are represented in Figure Figure 16.

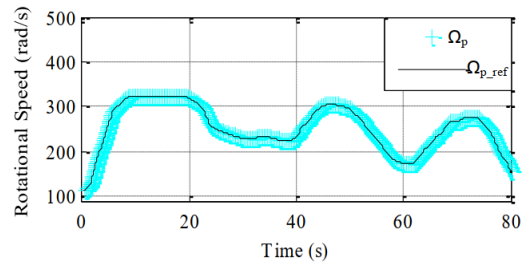


Figure 15: Rotational speed and its reference of the IM

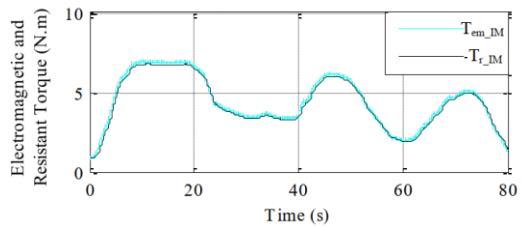


Figure 16: Electromagnetic and Resistant Torque of the IM

The direct and in quadratic rotor fluxes are shown in Figure Figure 17. The latter is zero, which justifies the reliability of the developed control.

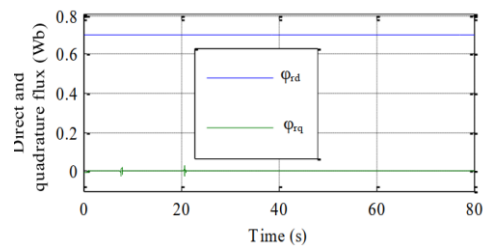


Figure 17: Rotor, direct and in quadratic flux of the IM ($\phi = 0.7 \text{ Wb}$)

The voltage and current of the IM stator phase are shown in figure 18. The zoom on a period illustrated in the same figure shows the motor mode operation of the induction machine.

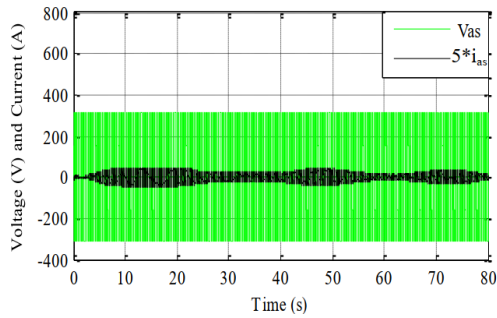


Figure 18: Stator, Voltage and Current of the IM

4.2. Elimination of the power electronics bay

In this part, the model established and represented in the system of equations (31), was implemented under the MATLAB / Simulink environment and a calculation code is obtained. The simulation results illustrated in figures ranging from 19 to 25, are obtained with a resistance torque motor-centrifugal pump $T_r = K_r W_p^2$. This one is directly powered by the passive stall wind generator.

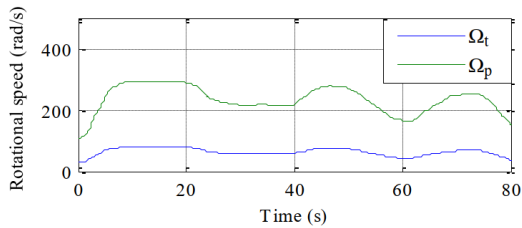


Figure 19: Rotational speed

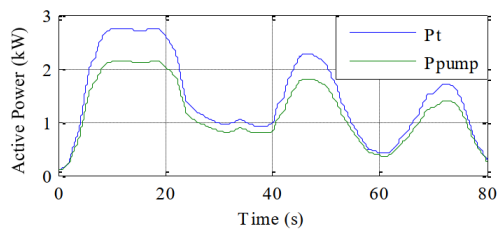


Figure 20: Turbine and Pump Active Powers

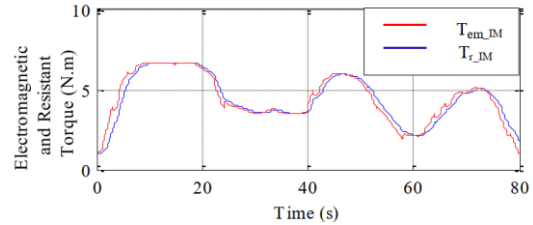


Figure 21: Electromagnetic and Resistant Torque of the IM

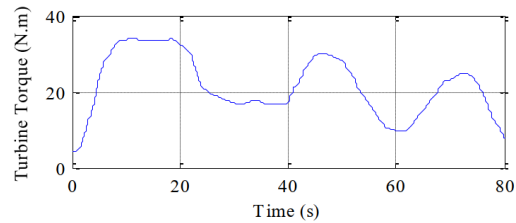


Figure 22: Turbine Torque

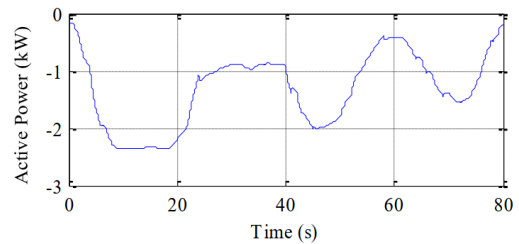


Figure 23: Active Power of the PMSG

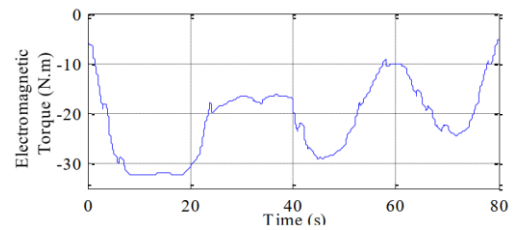


Figure 24: Electromagnetic Torque of the PMSG

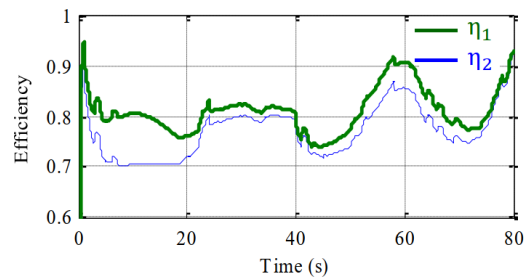




Figure 25: Efficiency of the global system with and without converter

Figures from Figure 19 to Figure 24 represent respectively:

- The evolution of the rotational speeds of the wind turbine and of the motor pump,
- The powers of the turbine and of the motor pump,
- The pump resistance torque and the IM electromagnetic torque,
- The mechanical torque of the turbine,
- Active power and PMSG electromagnetic torque.

Through these results, one concludes that; on the one hand, the profiles of rotational speed, torque and active power of the wind generator are images of the same profiles of the motor pump. The wind generator operating instructions are imposed by the motor pump, and within the limits imposed by the pumping system. Hence the master-slave operation; (motor pump (master), wind generator (slave)), on the other hand, it was shown the right operation of the pumping system on two zones, namely:

Zone where passive stalling is active, over the time interval ranging from 8 to 22 seconds.

Zone where the power production is partial, and this is outside the interval corresponding to the operating zone where the passive stall is activated.

The efficiency of the overall system h_1 with the presence of the static converter turns around 0.8; while the overall efficiency h_2 with elimination of the power electronics bay is

slightly degraded as shows Figure Figure 25; this is due to the choice of the centrifugal pump. As a consequence, on the one hand, the system is less bulky; on the other hand, the system has become simpler, less expensive and requires less maintenance.

5 Conclusion

The aim of this article was to examine the performance improvement of wind pumping system using a centrifugal pump. The main contribution lies in eliminating the possibility of the power electronics bay, in order to make the system less bulky, requiring less maintenance, reducing the cost of the pumping, and eliminating harmonics caused by the power electronics interface.

Models of the pumping system with and without power electronic converter have been established and implemented for simulation tests. The obtained results have clearly shown, on the one hand, that the wind generator follows the power demand required by the motor pump, hence the emphasis on the master-slave operation. Wind pumping with elimination of the power electronics bay is made possible only with the centrifugal pump. It has been shown that the overall efficiency of the system is slightly degraded; moreover, this degradation is more significant for high wind speed, due to the choice of the pump. Indeed, an adequate adaptation of the torque-speed characteristic of the centrifugal pump contributes to the right functioning of the wind pumping system, confirming therefore the reliability of the proposed model.

References

- [1] Z. Al «Wind-Powered electric Water-pumping system installed in a remote location», Applied Energy, 65,339 ± 34, 2000.
- [2] O. Badran Al «Wind turbine utilization for Water pumping in Jordan», Journal wind Engineering and Industrial Aerodynamics, 91, 1203-1214, 2003.
- [3] C. Evangelista, and Al «Lyapunov-Designed Super-Twisting Sliding Mode Control for Wind Energy Conversion Optimization», IEEE Transactions on Industrial Electronics, vol. 60, no. 2, 2013.



- [4] T. Ghennam, and Al «Advanced Control System of DFIG based Wind Generators for reactive Power Production and Integration in a Wind farm dispatching», *Energy Conversion and Management*, 105, 240-250, 2015.
- [5] S. Ghodelbourk, and Al «New techniques to improve the power control in the double-fed induction generator wind turbine», *Wind Engineering*, February , 2016.
- [6] F.Abdoune, and Al « Terminal voltage build-up and control of a DFIG based stand-alone wind energy conversion system », *Renewable Energy* 97, 468,480, 2016.
- [7] R.Pereira, and Al «Active stall control for large offshore horizontal axis wind turbines; a conceptual study considering different actuation methods», *Journal of Physics: Conference Series* 555, 012082, 2014.
- [8] B.S. Pali, S. Vadhera «A novel pumped hydro-energy storage scheme with wind energy for power generation at constant voltage in rural areas», *Renewable Energy* 127, 802-810, 2018.
- [9] R.N. Clark, K.E. Mulk «Water Pumping for livestock», *Wind Power Proceedings, USA*, 1992.
- [10] F.Amrane, A.Chaiba, S.Mekhilef «High performances of Grid-connected DFIG based on Direct Power Control with Fixed Switching Frequency via MPPT Strategy using MRAC and Neuro-Fuzzy Control», *Journal of Power Technologies* 96, (1), 2016.
- [11] A.Chenna, D.Aouzellag, K.Ghedamsi « Study and Control of a Pumped Storage Hydropower System Dedicated to Renewable Energy Resources», *Journal Européen des Systèmes Automatisés*. Vol.53, No.1. PP. 95-102. February, 2020.
- [12] H.Iman-Eini, D.Frey, S.Bacha, C.Boudinet, and J-L.Schanen «Evaluation of Loss Effect on Optimum Operation of Variable Speed Micro-hydropower Energy Conversion Systems», *Renewable Energy* Vol.131, PP.1022-1034. February, 2019.
- [13] F.Amrane, A.Chaiba, S.Mekhilef «High performances of Grid-connected DFIG based on Direct Power Control with Fixed Switching Frequency via MPPT Strategy using MRAC and Neuro-Fuzzy Control» *Journal of Power Technologies* 96 (1) PP. 27-39. 2016.
- [14] S. Taraft, D. Rekioua, D. Aouzellag, S. Bacha «A proposed strategy for power optimization of a wind energy conversion system connected to the grid» *Energy Conversion and Management* 101 PP. 489–502, 2015.
- [15] S. Taraft, D. Rekioua, D. Aouzellag, «Performances Study of the DFIG Associated to the Variable Speed Wind Turbine Connected to the Grid» *International Journal of Electrical and Power Engineering* 2 (5) , PP.353-364, 2008.